Weather Clim. Dynam., 6, 1015–1026, 2025
https://doi.org/10.5194/wcd-6-1015-2025

Weather and Climate Dynamics
Open Access
EGU

The impact of tropospheric blocking on the duration of the sudden stratospheric warmings in boreal winter 2023/24

Ekaterina Vorobeva and Yvan Orsolini

NILU – The Climate and Environmental Research Institute, Kjeller, Norway

Correspondence: Ekaterina Vorobeva (evor@nilu.no)

Received: 28 February 2025 – Discussion started: 7 March 2025
Revised: 16 June 2025 – Accepted: 7 July 2025 – Published: 26 September 2025

Abstract. The winter of 2023/24 exhibited remarkable stratospheric dynamics with multiple sudden stratospheric warmings (SSWs). Based on the fifth-generation European Centre for Medium-Range Weather Forecasts (ECMWF) reanalysis (ERA5) polar-cap-averaged 10 hPa zonal wind, three major SSWs are identified. Two of the three SSWs were short-lived, lasting under 7 d. In this study, we give an overview of the three SSWs that occurred in the winter of 2023/24 and focus on the impact of tropospheric forcing on their duration. Blocking high-pressure systems are shown to modulate wave activity flux into the stratosphere through interactions with tropospheric planetary waves, depending on their location. The rapid termination of the first SSW (14–19 January 2024) is linked to a developing high-pressure system over the North Pacific. The second SSW (16–22 February 2024) terminated quickly due to more contributing factors, one of which was a high-pressure system that developed over the Far East. The third SSW (3–28 March 2024) was a long-duration canonical event extending to levels below 100 hPa. In contrast to the two short-lived SSWs in the winter of 2023/24, tropospheric forcing was sustained around the SSW onset in March 2024, allowing a long event to develop. We also note that conditions for these SSWs were particularly favorable due to external factors, including an easterly Quasi-Biennial Oscillation (QBO), the presence of El Niño conditions of the El Niño–Southern Oscillation (ENSO) cycle, and the proximity to the solar maximum.

1 Introduction

The wintertime high-latitude stratospheric circulation is characterized by prominent eastward winds encircling the pole and spanning ~ 100 to over 1 hPa, also known as the stratospheric polar vortex. The prevailing wintertime stratospheric wind pattern is regularly disturbed by planetary waves (PWs) originating from the troposphere (Matsuno, 1970). Extreme examples of the stratospheric polar vortex disturbance by PWs are sudden stratospheric warmings (SSWs) (see, e.g., Waugh and Polvani, 2010; Charlton and Polvani, 2007). According to previous studies (see, e.g., Limpasuvan et al., 2004, 2016; Shepherd et al., 2014, and references therein), SSWs originate in the upper mesosphere at high latitudes and extend downwards into the stratosphere at high latitudes, before extending further into lower latitudes. SSWs can be classified into minor and major events, based on either a temporary weakening or a reversal of stratospheric winds to a summer-like westward regime, and into split and displacement events, based on the spatial structure of the disturbed stratospheric polar vortex. Based on the classical definition of SSWs by Charlton and Polvani (2007), major events tend to occur around six to seven times per decade (Baldwin et al., 2021), as also confirmed by model simulations (Rao and Garfinkel, 2021). However, their frequency of occurrence can vary significantly on inter-annual to decadal timescales (Butler et al., 2017).

Most definitions of SSW onset are based on stratospheric zonal-mean zonal wind and temperature at 10 hPa (see, e.g., Butler et al., 2015; Baldwin et al., 2021, for reviews). However, it is important to note that these dramatic disruptions of atmospheric circulation impact the entire atmospheric column, from the troposphere to the thermosphere across diverse latitudinal ranges (see, e.g., Limpasuvan et al., 2016; Pedatella, 2023; Liang et al., 2022). Duration wise, the eastward wind reversal (typically at 10 hPa) during major SSWs displays remarkable diversity, ranging from short events

(lasting only a few days) to more canonical long-lasting events (lasting over several weeks). Previous studies have demonstrated that long SSW events may affect tropospheric weather and climate patterns. The impacts include the occurrence of cold-air outbreaks across North America and Eurasia (Kolstad et al., 2010), shifts in the jet stream southward over the Euro-Atlantic region, and a negative phase of the North Atlantic Oscillation (Butler et al., 2017).

Recent studies have emphasized the critical role of tropospheric blocking in stratospheric variability. Blocking events, characterized by persistent high-pressure systems (hereafter blocking highs or BHs) that disrupt the typical eastward flow, can act as a precursor to SSWs by influencing PW propagation into the stratosphere (e.g., Martius et al., 2009; Bancalá et al., 2012; Nishii et al., 2011). The geographical positioning of BHs prior to SSW onset has been studied in the context of SSW types, intensity, and duration. Martius et al. (2009) and Bancalá et al. (2012) found a strong relation between the SSW spatial type and the geographical location of BHs in the troposphere, with displacement events being associated predominantly with BHs in the Euro-Atlantic sector (where a climatological PW ridge is located) and split events linked to BHs either in the Pacific sector (climatological PW trough) or simultaneously across both the Atlantic and the Pacific sectors. Nishii et al. (2011) and Ayarzagüena et al. (2015) demonstrated that BHs over the Euro-Atlantic region tend to increase upward propagation of planetary waves and cause the weakening of the polar vortex, whereas BHs over the western Pacific and Far East suppress the upward propagation of planetary waves and lead to a stronger polar vortex. Orsolini et al. (2018) showed that the synoptic evolution of BHs around onset is a critical parameter determining the SSW duration. BHs situated over the Euro-Atlantic sector are often associated with prolonged SSWs by sustaining the upward wave activity flux, whereas those developing over the western Pacific sector may contribute to the short duration and termination of SSWs by lowering the wave activity flux.

In the winter of 2023/24, the stratospheric polar vortex was weak and highly variable, and multiple SSWs took place. Following the classical definition of SSWs (Charlton and Polvani, 2007) and using the fifth-generation European Centre for Medium-Range Weather Forecasts (ECMWF) reanalysis (ERA5), a recent study by Lee et al. (2025) identified two major SSWs. This occurrence in one winter was last seen in 2010 and is rather uncommon (Ineson et al., 2024). This unusual event has attracted the attention of the scientific community and has led to publications on various aspects of stratospheric dynamics in the winter of 2023/24. Lee et al. (2025) provided a general overview of winter conditions, summarizing the evolution of the SSWs, and paid attention to their surface impact. Qian et al. (2024) focused on the coupling between the stratosphere and troposphere and between the tropics and the Arctic. Rao et al. (2025) used the disturbed stratospheric dynamics of the winter of 2023/24 to study the impact of frequent SSWs on the predictability of near-surface conditions.

Despite extensive prior research on the predictability of SSWs, it remains an open question why some SSWs develop into long events while others terminate quickly. Addressing this question is the main focus and novel aspect of this paper: the winter of 2023/24 presented a beneficial scenario due to the occurrence of multiple SSWs of different durations within 3 months. Three major SSWs are identified in the winter of 2023/24 using a definition based on polar-cap-averaged zonal wind derived from ERA5 reanalysis data. Two short-lived events and one long-lived event occurred on 14 January, 16 February, and 3 March 2024, respectively. In this study, we give an overview of these SSWs and focus on the impact of tropospheric forcing on their duration. For all three SSW events, it is demonstrated that blocking highs developing over the PW ridges were indeed responsible for the enhanced PW activity prior to the onset of SSW. The short duration of SSWs in January and February 2024 was shown to be the result of the blocking highs developing in the PW trough over the western Pacific/Far East, which suppressed PW activity and caused the quick termination of these events. In contrast, the persistent blocking highs over the Euro-Atlantic sector sustained the upward wave activity flux, allowing for a long SSW in March 2024.

The data and methods used in this study are introduced in Sect. 2. Analysis of multiple SSWs in the winter of 2023/24 and insights into their tropospheric forcing are presented in Sect. 3. The results obtained are further discussed in Sect. 4.

2 Data and methods

In this study, atmospheric data are obtained from the ECMWF ERA5 reanalysis with 1 h temporal and $0.25° \times 0.25°$ spatial resolution. Open-access ERA5 data are available on 37 pressure levels up to 1 hPa. For an overview of the ERA5 strengths, biases, and validation, we refer to Hersbach et al. (2020) and Bell et al. (2021).

To assess the stratospheric state and its interaction with the troposphere, the following atmospheric data are used: air temperature (T), zonal and meridional winds (U and V), and geopotential height (z) at all available pressure levels from 1000 to 1 hPa. The aforementioned variables are extracted from the open-access ECMWF archive (Hersbach et al., 2023) (see data availability statement) and averaged daily. Daily climatological means for T, U, V, and z are calculated based on 2000–2022 ERA5 data. For the leap years, 29 February is not considered.

To analyze tropospheric forcing, we calculate the meridional eddy heat flux, $v'T'$, which is directly related to the upward wave activity flux from the troposphere into the stratosphere (Newman and Nash, 2000). Here, the prime symbol denotes the deviation from the zonal mean. When zonally averaged, the eddy heat flux is proportional to the ver-

tical component of the Eliassen–Palm (E–P) flux (Andrews et al., 1987). Previous studies have shown that increased (reduced) meridional eddy heat flux may weaken (strengthen) the stratospheric polar vortex (see, e.g., Coy et al., 1997; Newman et al., 2001; Matthias et al., 2016). It is, therefore, often used as a precursor for weak and strong polar vortex events (Polvani and Waugh, 2004). Typically, $v'T'$ is calculated at 100 hPa. Hinssen and Ambaum (2010) demonstrated that nearly half of the year-to-year variations in the Northern Hemisphere stratosphere are influenced by fluctuations in the heat flux at 100 hPa. The contribution to the meridional eddy heat flux by individual waves is calculated by multiplying the corresponding Fourier components of v' and T' (Newman and Nash, 2000). Thus, the zonal wavenumber 1 component of $v'T'$ is calculated as $v'T'_{\mathrm{wv}=1} = v'_{\mathrm{wv}=1}T'_{\mathrm{wv}=1}$. In this study, we consider the meridional eddy heat flux, area averaged poleward of 45° N (hereafter $[v'T']$).

Various criteria exist to determine the onset of an SSW (Butler et al., 2015). The commonly used definition is based on the reversal of the zonal-mean U at 60° N and 10 hPa, as proposed by Charlton and Polvani (2007). However, Butler and Gerber (2018) focused on optimizing the definition of SSW and concluded that features of major SSWs are maximized between 55 and 70° N in the middle stratosphere (30–5 hPa). Therefore, one can miss short and weak major SSW events that do not have enough time to extend to 60° N when using the classical definition (an example is shown below for mid-February 2024). For this reason, the SSW onsets in this study are obtained based on the time series of 10 hPa U area averaged poleward of 60° N (hereafter polar-cap averaged), allowing one to assess the polar stratospheric dynamics without focusing on one specific latitude. Note, however, that the choice of SSW definition affects its reported frequency of occurrence. Butler et al. (2015) showed that the occurrence rate is around eight to nine events per decade when using the polar-cap-averaged zonal wind compared to six to seven events per decade when using the classical SSW definition (Charlton and Polvani, 2007). Moreover, the reanalysis record indicates that winters with two SSW events are more common when using the polar-cap-averaged definition and that at least one winter with three SSWs has occurred (see Fig. 2 in Butler et al., 2015). SSW onset is defined as the day when daily-mean polar-cap-averaged U turns westward and its duration corresponds to the number of days it remains westward.

3 Results

3.1 Onset and duration

As mentioned in Sect. 1, SSW signatures emerge primarily at the high latitudes and extend toward the middle latitudes. Therefore, we focus on analyzing the latitude–time cross-section of the zonal-mean T and U at 10 hPa during December 2023–April 2024 (Fig. 1). Figure 1 also shows the time series of the zonal-mean 10 hPa T and U at 60 and 65° N and polar-cap-averaged T and U at 10 hPa. Similar latitude–time cross-sections, based on ERA5 data, were shown by Qian et al. (2024), but our U line plot (Fig. 1d) shows that the choice of a threshold latitude determines whether the mid-February event is classified as a major or minor SSW.

At the end of December 2023, the polar vortex exhibited signs of weakening across a broad band of latitudes, nearly reversing its flow at the pole (Fig. 1c). Due to the lack of a westward reversal, this weakening does not qualify as an SSW, although it played a key role in the unusually early generation of the 2 d wave in the austral hemisphere (Qin et al., 2025). During the first week of January 2024, the temperature exceeded 240 K near the pole; however the westward zonal-mean U did not reach mid-latitudes. Soon after, the zonal-mean U reversed to a westward regime around the pole once again and spread towards 60° N within the following days. At 60° N, the zonal-mean U remained westward for 2 d only (blue curve in Fig. 1d), while the polar-cap-averaged U remained westward until 20 January 2024. Recovery of the polar vortex began thereafter, with the vortex returning to its climatological mean by 24 January 2024 and intensifying in the following 2 weeks. We identify the SSW in January 2024 as a major event with onset on 14 January 2024, which lasted for 6 consecutive days.

On 15 February 2024, the zonal-mean U reversed at the pole, and the westward U spread towards mid-latitudes within the following days (Fig. 1c). In this case, using the standard SSW definition would identify the February SSW as a minor SSW (see, e.g., Qian et al., 2024; Rao et al., 2025; Lee et al., 2025) as it did not have enough time to extend its signatures to 60° N (Fig. 1d). However, we argue that the SSW in February 2024 was clearly associated with an increased temperature exceeding 230 K and a reversal of zonal-mean U in a broad range of latitudes over the course of around 1 week (Fig. 1a and c). By the end of February 2024, the polar vortex returned to its climatological mean. Based on the polar-cap-averaged definition, we identify the SSW in February 2024 as a major event with onset on 16 February 2024, which lasted for 7 consecutive days.

Figure 1a and c show a nearly simultaneous reversal of the zonal-mean U in the 50–90° N band and the associated increase in the zonal-mean T values over 230 K on 3 March 2024. Compared to the SSWs in January and February 2024, the SSW in March 2024 was a long-lasting event with polar-cap-averaged U reaching below $-20\,\mathrm{m\,s^{-1}}$, close to the absolute minimum in the 2000–2022 period (Fig. 1d). We conclude that the SSW in March 2024 was a major event with onset on 3 March 2024, which lasted for 26 consecutive days. This event is considered major warming rather than final warming as U returned to its eastward regime well prior to the end of April.

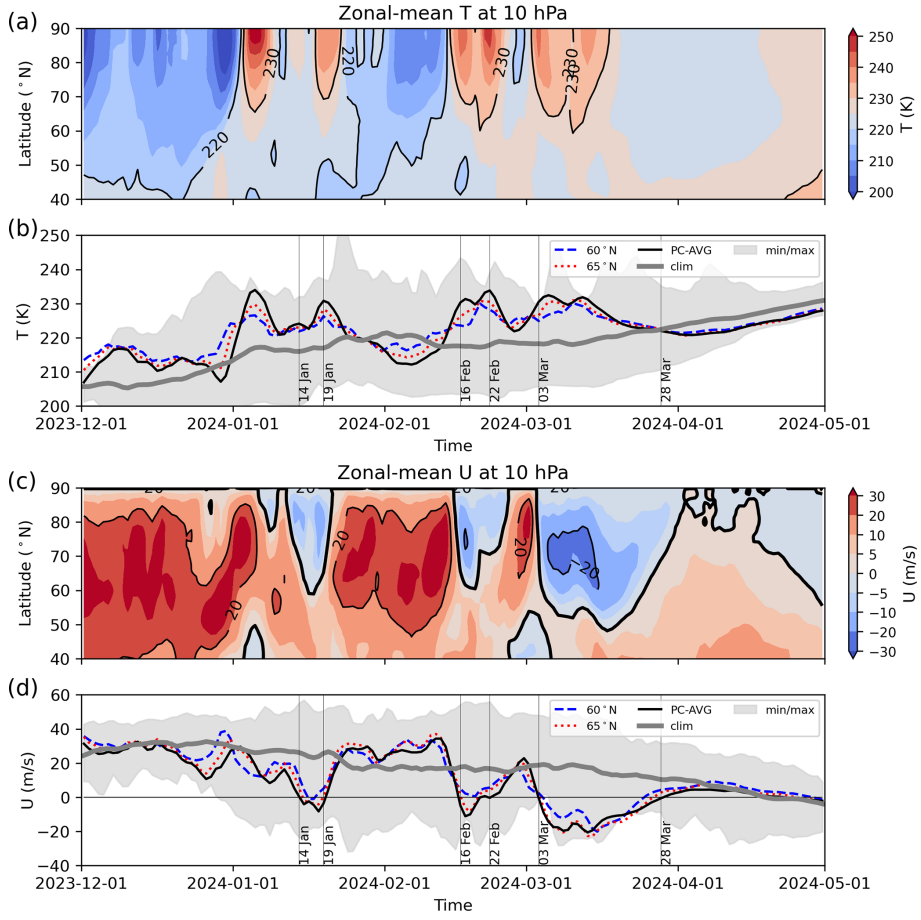

Figure 1. Latitude–time cross-section of zonal-mean **(a)** temperature, T (K), and **(c)** zonal wind, U ($\mathrm{m\,s^{-1}}$), at 10 hPa during December 2023–April 2024. The thick black contours in **(c)** indicate zero wind. The associated time series of the zonal-mean **(b)** temperature and **(d)** zonal wind at 60° N (blue dashed), at 65° N (red dotted), and area averaged poleward of 60° N (PC-AVG, black solid). Climatological means for the polar-cap-averaged T and U are plotted as thick gray curves, and the min–max range is shaded based on 2000–2022 ERA5 data.

3.2 Vertical structure of zonal wind and heat flux and their evolution

This section focuses on the altitude–time evolution of the polar-cap-averaged U and meridional eddy heat flux in the winter of 2023/24. Figure 2a shows that the polar-cap-averaged U reversed to the summer-like westward regime three times in the upper stratosphere in January 2024. First, the 1 hPa polar-cap-averaged U reversed on 2 January 2024 and caused weakening of 10 hPa polar-cap-averaged U around 5 January 2024, as is also seen in Fig. 1. At 10 hPa, polar-cap-averaged U reversed on 14 January 2024 and remained westward until 20 January 2024, while two separate episodes of 1 hPa polar-cap-averaged U reversal on 11–14 and 17–21 January 2024, which reached down to around 20 hPa, can be seen. In February 2024, the polar-cap-averaged U reversal occurred nearly simultaneously in a deep layer of 20–1 hPa. By 24 February 2024, polar-cap-averaged U returned to the eastward regime. Nevertheless, above 10 hPa, U did not reach the anomalously strong intensity it had in early February. Hence, the stratospheric polar circulation became preconditioned for the March SSW. In March 2024, polar-cap-averaged U reversed in the entire stratosphere (100–1 hPa). From Fig. 2a, it can be seen that the westward polar-cap-averaged U lasted longer at the 10 hPa pressure level (up to 29 March 2024), while 1 hPa polar-cap-averaged U returned to the eastward regime already on 16 March 2024. One can also see two episodes of the westward polar-cap-averaged U intensification located at slightly different pressure levels that are separated in time by approximately a week. Another interesting feature seen here is that the short-lived SSW in January 2024 was more intense than the long SSW in March 2024 at 1 hPa.

Orsolini et al. (2018) investigated the differences between short- and long-lived SSWs in the ECMWF seasonal forecast model. They showed that despite the fact that the westward U penetrates as deeply as in long events right at their onset, short events decay rapidly due to a wave forcing that is less

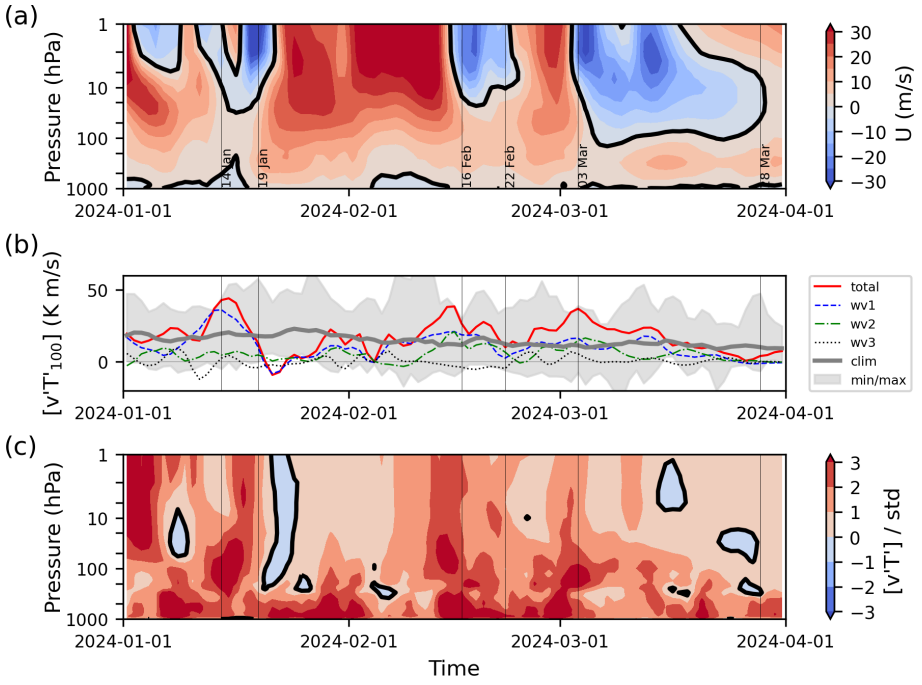

Figure 2. **(a)** Time–pressure cross-section of the polar-cap-averaged zonal wind, U ($\mathrm{m\,s^{-1}}$), during January–March 2024. The thick black contours indicate zero wind. **(b)** The 100 hPa meridional eddy heat flux area averaged poleward of 45° N, $[v'T'_{100}]$ ($\mathrm{K\,m\,s^{-1}}$) (total, solid red), for the same period. Zonal wavenumber 1 (wv1, dashed blue), wavenumber 2 (wv2, dashed–dotted green), and wavenumber 3 (wv3, dotted black) components of the heat flux are calculated as described in Sect. 2. Climatological mean is plotted as the thick gray curve, and the min–max range is shaded based on 2000–2022 ERA5 data. **(c)** Time–pressure cross-section of the total meridional eddy heat flux area averaged poleward of 45° N, $[v'T']$ ($\mathrm{K\,m\,s^{-1}}$), and normalized by its standard deviation, std ($\mathrm{K\,m\,s^{-1}}$), at each pressure level. The thick black contours indicate zero values. The vertical lines indicate the onsets and duration of the three SSWs obtained in Sect. 3.1.

sustained than during long events. In contrast, long events continue to develop, strengthening westward U throughout a deepening stratospheric layer. Both the near-simultaneous deceleration of all three SSWs in a deep stratospheric layer down to 20 hPa regardless of duration, shown in Fig. 2a, and the persistence of the lower-stratospheric eddy forcing in March, shown in Fig. 2b and c, are in agreement with Orsolini et al. (2018).

Figure 2b shows time series of the 100 hPa meridional eddy heat flux area averaged poleward of 45° N. One can see three episodes of the increased and sustained heat flux that are collocated in time with the onsets of the three SSWs. Anomalously strong meridional eddy heat flux at 100 hPa is known to nearly always precede weak vortex events (including SSWs), consistent with wave–mean flow interaction theory (Polvani and Waugh, 2004; Karpechko et al., 2017). Sjoberg and Birner (2012) found that forcing duration has an even greater influence on SSW generation than forcing amplitude. This agrees with Fig. 2b, where the 100 hPa meridional eddy heat flux had increased values compared to its climatological mean for several days prior to the onsets. Karpechko et al. (2017) also found that SSWs are more likely to have a tropospheric impact when the wave forcing at 100 hPa is sustained for several days after the onset. A recent study by Qian et al. (2024) analyzed stratosphere–troposphere coupling in the winter of 2023/24 and found that all three SSWs were associated with positive geopotential height anomalies propagating down to the troposphere and the surface. This agrees well with the meridional eddy heat flux anomaly at 100 hPa remaining positive for more than 5 d after the onsets, as seen in Fig. 2b.

In January 2024, the zonal wavenumber 1 component of the 100 hPa meridional eddy heat flux had the largest contribution around the SSW onset, while the zonal wavenumber 1 and 2 components had a comparable contribution around the SSW onset in February 2024. In March 2024, two peaks in the 100 hPa meridional eddy heat flux, corresponding to the two previously mentioned episodes of strong westward intensification of the polar-cap-averaged U in the stratosphere, are seen in Fig. 2a. At the first peak, the zonal wavenumber 1 and 2 components had a nearly equal contribution, while the zonal wavenumber 1 component dominated at the second peak. The relative contribution of the zonal wavenumber 1 and 2 components is often associated with the SSW type in the literature (see review by Baldwin et al., 2021, and references therein). Wavenumber 1 activity is typically associated with displacement SSWs, where the polar vortex is shifted off the pole, while wavenumber 2 activity is often linked to

split SSWs, where the polar vortex is divided into smaller vortices. Despite the presence of wavenumber 2 pulses in the 100 hPa meridional eddy heat flux prior to the SSWs in February and March 2024, the recent study by Qian et al. (2024) classified all three SSWs in the winter of 2023/24 as displacement events based on the analysis of 10 hPa geopotential height time series.

The temporal evolution of the 100 hPa meridional eddy heat flux in January 2024 largely follows the life cycle of a short-lived SSW, as described in Orsolini et al. (2018). Such events are characterized by a significant increase in the meridional eddy heat flux prior to the SSW onset, followed by a quick transition to values much lower than the climatological mean a few days after. Notably, the absolute values of the total meridional eddy heat flux became negative after the SSW onset in January 2024, possibly indicating a reflection of PWs in the lower stratosphere. To highlight the location of a region where the total meridional eddy heat flux was negative, Fig. 2c shows the total meridional eddy heat flux area averaged poleward of 45° N and divided by its standard deviation at each pressure level as a function of pressure and time. Negative values within 1 standard deviation spread from $\sim$ 200 to 1 hPa within the following days. This could dynamically accelerate the recovery of stratospheric circulation and may be the reason for the rapid termination of the SSW in January 2024. More details on the tropospheric forcing behind the negative meridional eddy heat flux are provided in Sect. 3.3.

Figure 2c also indicates several episodes of the negative meridional eddy heat flux in March 2024. In mid-March, negative values were localized between 5 and 1 hPa around the time when the polar-cap-averaged U returned to positive values in the upper stratosphere (Fig. 2a). At the end of March, negative values of the total meridional eddy heat flux appeared in the lower stratosphere between 70 and 20 hPa. It is evident from Fig. 2a that the westward polar-cap-averaged U began to weaken around this time and returned to the eastward regime quickly after.

3.3 Tropospheric forcing

Blocking high-pressure systems play a significant role in modulating large-scale atmospheric flow, particularly through their interactions with tropospheric planetary waves, and controlling the wave activity flux into the stratosphere (Nishii et al., 2010; Woollings et al., 2010). As mentioned in Sect. 1, such interactions have an impact on the strength of the polar vortex based on the geographical location of BHs. Numerous blocking indices have been proposed in the literature to identify the blocking events, and the results obtained using these indices can differ (Martius et al., 2009; Woollings et al., 2010). In this study, we define blocking events as large (> 0.2 km) and persistent (> 3 d) positive anomalies of 200 hPa geopotential height, and the meridional eddy heat flux $v'T'$ is decomposed following Nishii et al. (2011) as

$$v'T' = v'_c T'_c + v'_a T'_c + v'_c T'_a + v'_a T'_a, \quad (1)$$

where the sub-indexes c and a denote the climatological mean and anomalies. Here, the first term corresponds to the meridional eddy heat flux due to the climatological PWs. The second and third terms are linear interference terms that correspond to interactions between the climatological PWs and anomalies. The last term is a nonlinear term.

The meridional eddy heat flux $v'T'$ consists of climatological mean, $(v'T')_c$, and anomaly components, $(v'T')_a$. Following Nishii et al. (2009), $(v'T')_c$ and $(v'T')_a$ are expressed as

$$(v'T')_c = v'_c T'_c + (v'_a T'_a)_c \quad (2)$$

and

$$(v'T')_a = v'_a T'_c + v'_c T'_a + (v'_a T'_a)_a. \quad (3)$$

From Eqs. (2) and (3), it is clear that the climatology of the nonlinear term contributes to the meridional eddy heat flux climatology, while the anomaly component of the nonlinear term contributes to the anomalous meridional eddy heat flux.

To demonstrate the impact of the BH geographical location on the upward PW propagation variability, Fig. 3 shows the 200 hPa geopotential height anomalies together with the anomalous 100 hPa meridional eddy heat flux (see Eq. 3) in three 4 d windows around the SSW onsets in the winter of 2023/24. Deviations of the climatological mean 200 hPa geopotential height from its zonal mean are also shown to highlight climatological PW ridges and troughs.

Prior to the SSW in January 2024, a large-scale BH was present over the North Atlantic and Greenland and partially over the Arctic Ocean, partially covering two PW ridges and one trough over northern Canada (Fig. 3a). The associated regions of positive (purple contours) and negative (green contours) anomalous meridional eddy heat flux were observed. As seen in Fig. 2b, the combined effect resulted in the increased 100 hPa meridional eddy heat flux area averaged poleward of 45° N. In the following 4 d, the BH began to separate into two smaller systems located over the PW troughs in the Arctic Ocean and the North Pacific, causing a reduction in the meridional eddy heat flux (Figs. 3b and 2b). Around 5–8 d after the onset, the BH over the Arctic Ocean decayed, while the BH over the North Pacific was sustained and migrated westward, deeper into the PW trough (Fig. 3c), further developing a negative anomalous meridional eddy heat flux. Hence, the latter constituted the largest contribution to the zonal-mean negative heat flux (Fig. 3c). There is also a smaller negative contribution over central Eurasia, but the contribution from the North Atlantic sector is weakly positive. At this time, the absolute value of the 100 hPa meridional eddy heat flux turned negative, as indicated in Fig. 2b. It has already been mentioned in Sect. 3.2 that negative values of the meridional eddy heat flux spread throughout the

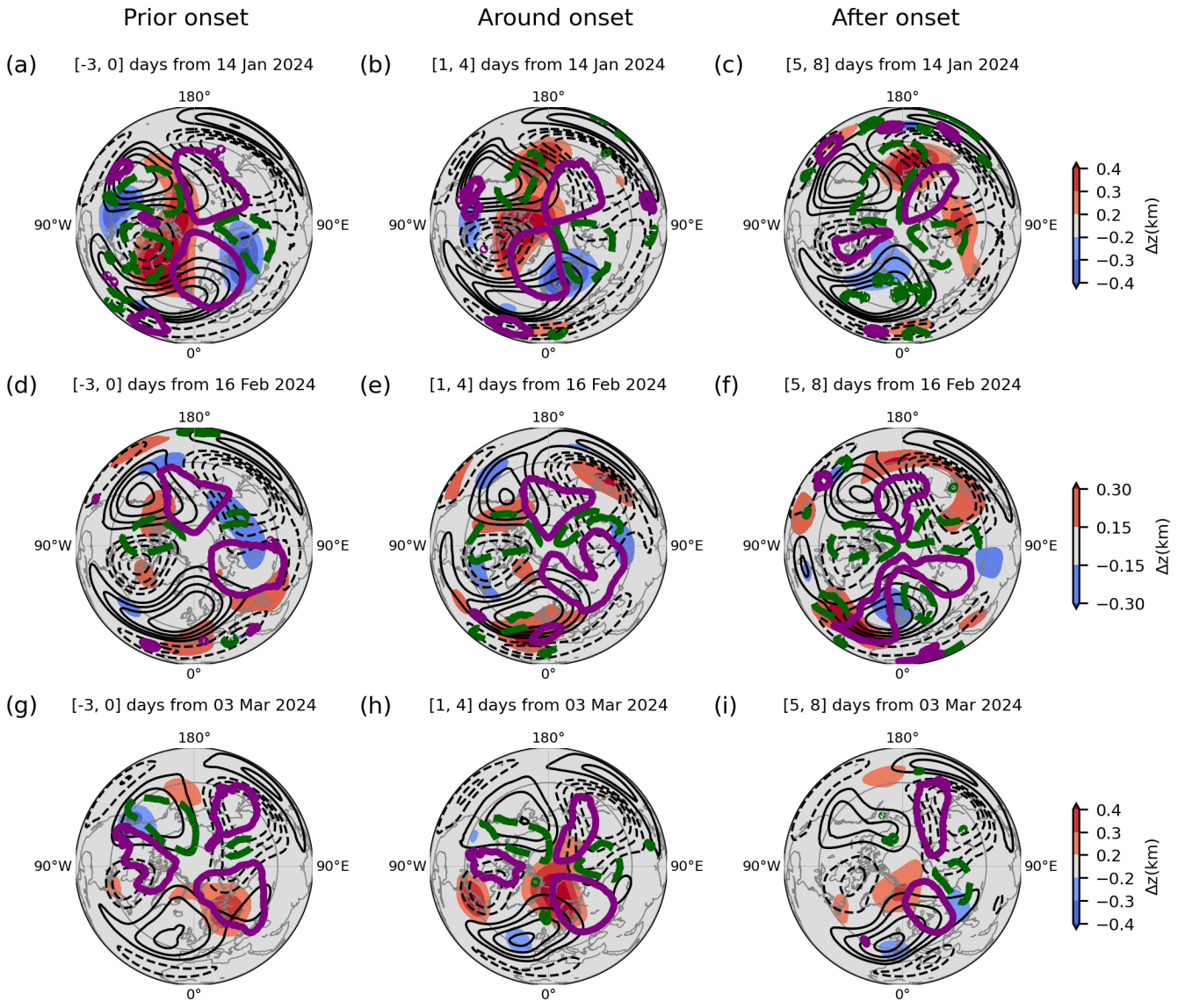

Figure 3. Tropospheric forcing conditions around SSW in **(a)** January, **(d)** February, and **(g)** March 2024 for three 4 d windows around the onsets: **(a, d, g)** days −3 to 0, **(b, e, h)** days 1 to 4, and **(c, f, i)** days 5 to 8. The 200 hPa geopotential height anomalies, Δz (km), are shaded. Note that panels have different scales. The thin solid (dashed) black contours indicate positive (negative) deviations of the climatological mean 200 hPa geopotential height from its zonal mean (contours $\pm 0.05, 0.1, 0.15, 0.2$ km). The thick solid purple (dashed green) contours indicate positive (negative) anomalous 100 hPa meridional eddy heat flux (see Eq. 3; contours $\pm 50\,\mathrm{K\,m\,s^{-1}}$). Latitude of 45° N is shown to indicate the area where the 100 hPa meridional eddy heat flux was averaged in Fig. 2.

entire stratospheric column (see Fig. 2c). We therefore conclude that the westward-propagating BH in the North Pacific suppressed the upward PW activity and was the reason for the quick termination of the SSW in January 2024. The above-described timeline is in agreement with a weak polar vortex case described in Orsolini et al. (2018).

In February 2024, tropospheric forcing conditions looked different, with several BHs being present prior to the SSW onset. However, only two of them were located within the area poleward of 45° N, namely a large BH over the PW ridge in Alaska and a small BH over the PW trough near Hudson Bay (Fig. 3d), favoring an increased meridional eddy heat flux. In the following days, a BH emerged over the lower edge of the East Asian PW trough (Fig. 3e), causing increased negative anomalies in the meridional eddy heat flux and a decrease in the total 100 hPa meridional eddy heat flux (Fig. 2b). Around the SSW termination, the BH over the Far East split into two systems (one moved deeper into the continent, and the other moved eastward toward the Pacific). The BH over the Far East lay within the PW trough and contributed to the negative anomalous heat flux (green contour in Fig. 3f). At the same time, the BH over the Pacific ex-

tended along 45° N and partially covered both the PW ridge and the PW trough. Around this time, the 100 hPa meridional eddy heat flux was reduced to its climatological values, as shown in Fig. 2b, allowing the polar vortex to strengthen. The presence of several high-pressure systems in February 2024 could also explain the zonal wavenumber 2 signal in Fig. 2b.

In contrast to the two short-lived SSWs in the winter of 2023/24, the forcing was more sustained around the onset of the SSW in March 2024, allowing a long SSW to develop (Fig. 3g–i). Prior to the SSW onset, three high-pressure systems were present poleward of 45° N: the BH in northern Europe along the eastern edge of the PW ridge, a weaker BH over the western edge of the PW ridge in Alaska, and a small BH near the Hudson Bay PW climatological trough. From Figs. 2b and 3g, it is clear that such geographical positioning of BHs was associated with an increased meridional eddy heat flux. Within the next 4 d, the BH over northern Europe strengthened and moved towards the Greenland Sea, while the BH near the Hudson Bay strengthened. Around 5–8 d after the onset, the two aforementioned high-pressure systems weakened but stayed relatively close to their original locations, sustaining the positive values of the anomalous meridional eddy heat flux and allowing the further development of the SSW (Fig. 3i). Similar to the February SSW, the presence of several high-pressure systems could explain the zonal wavenumber 2 signal in Fig. 2b. The above-described sustained tropospheric forcing agrees well with what was proposed for a long SSW (Orsolini et al., 2018; Karpechko et al., 2017; Sjoberg and Birner, 2012). Note that during and after the wind reversal in March, descending easterlies would have hindered vertical propagation of PWs into the upper stratosphere, and PWs would have become evanescent in the lower stratosphere (Fig. 2c). We therefore conclude that the persistent BH partially overlapping the PW ridge in northern Europe enhanced the PW activity and was favorable for the development of a canonical long SSW in March 2024.

3.3.1 Contributions to the eddy heat flux near the termination of the two short-lived SSWs in winter 2023/24

To further elucidate which terms dominated the anomalous meridional eddy heat flux and to decipher the roles of the background temperature and meridional wind, this section provides deeper insight into the tropospheric forcing conditions around the termination of the two short-lived SSWs in the winter of 2023/24. Figures 4 and 5 provide additional details on the respective contributions of the interference and nonlinear terms in Eq. (3) to the total anomalous meridional eddy heat flux around the termination of the SSWs in January and February 2024. The spatial patterns of these three terms, and of their sum, are shown in Fig. 4 for each SSW event (left and right columns) during a 4 d time window following onset (more specifically days 5–8). Note that the purple and green contours in Fig. 4g and h are the same as in Fig. 3. Inspection of Fig. 4 reveals that (i) both interference terms (first and second rows, respectively) can contribute to the total anomalous meridional eddy heat flux (fourth row), depending on geographical location, and sometimes in opposite ways, and (ii) the nonlinear term (third row) can also be equally important at some locations.

Figure 5 shows the time evolution of both the total anomalous meridional eddy heat flux (red curve), spatially averaged over middle and high latitudes, and the three contributing terms. Again, it can be seen in these spatial averages that the interference terms can have opposite, i.e., negative or positive, contributions and that the nonlinear term can dominate at times.

In January 2024, the $v'_a T'_c$ interference term appears to be responsible for the large negative anomaly of the meridional eddy heat flux (Figs. 4a and 5, blue curve) that dominates the zonal mean. The anomalous equatorward advection of the background (climatological) warm air over Alaska and the North Pacific combined with the poleward advection of the background cold air over western Eurasia is mainly responsible for the large negative anomaly of the meridional eddy heat flux (e.g., blue curve in Fig. 5). Note that the climatological temperature exhibits a clear wave 1 pattern.

There is less clarity regarding the SSW in February 2024. Figure 5 indicates that the spatially averaged magnitudes of the interference and nonlinear terms in Eq. (3) were all weak and of nearly equal importance in the termination phase. From Fig. 4b, d, and f, it is clear that anomalous meridional wind had a complex pattern, in agreement with the presence of multiple BHs in the troposphere, as described above. On the other hand, the spatial pattern of the anomalous temperature had a wave 1 pattern similar to the climatological mean (Fig. 4b and d). Hence, the near-zero values of the area-averaged anomalous meridional eddy heat flux in Fig. 5 largely resulted from the mutually canceling positive and negative contributions from the meridional wind fields across the North Pacific, Eurasia, the Euro-Atlantic, and North America.

4 Discussion and conclusions

It has previously been shown in the literature that the occurrence of SSWs is influenced by external factors, like the Quasi-Biennial Oscillation (QBO), the El Niño–Southern Oscillation (ENSO), the solar cycle, and anomalous snow cover (Rao et al., 2019; Baldwin et al., 2021). For example, during the easterly phase of the QBO, SSWs are shown to be more frequent, as the low-latitude stratospheric easterly winds promote a critical line for stationary planetary waves in the subtropics, allowing more disruptions of the polar vortex (also known as the Holton–Tan relationship). ENSO also plays a key role, with the SSW likelihood being increased in both El Niño and La Niña phases (Domeisen, 2019). How-

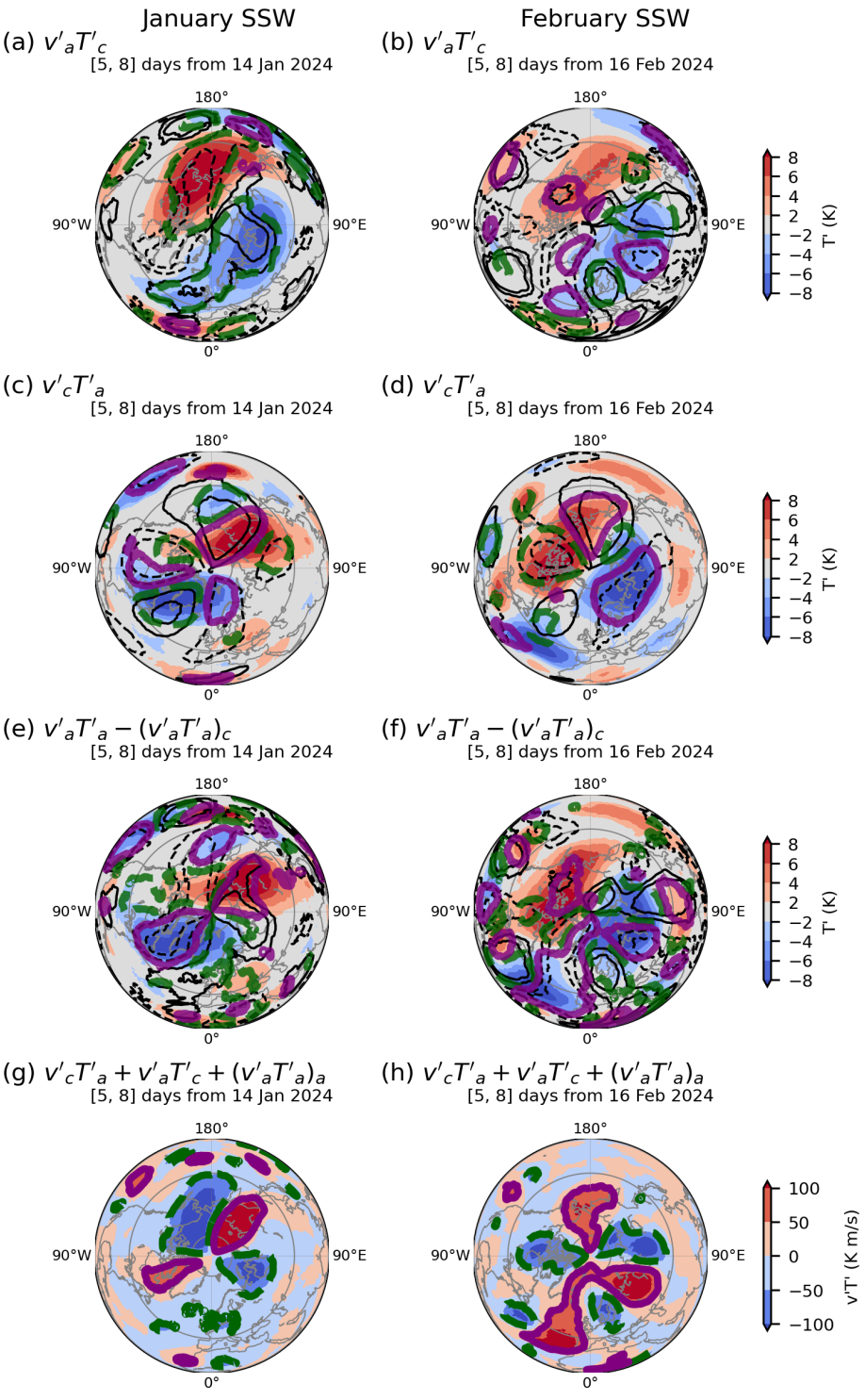

Figure 4. Details on the components of the anomalous meridional eddy heat flux in Eq. (3) around the SSW termination in January and February 2024. The thick solid purple (dashed green) contours of $\pm 20\,\mathrm{K\,m\,s^{-1}}$ indicate positive (negative) values of 100 hPa meridional eddy heat flux components: **(a, b)** $v'_a T'_c$, **(c, d)** $v'_c T'_a$, and **(e, f)** $(v'_a T'_a)_a$. The eddy temperature, T' (K), either climatological in **(a, b)** or anomalous in **(c–f)**, is shaded, and the eddy meridional wind, v' ($\mathrm{m\,s^{-1}}$), either climatological in **(c, d)** or anomalous in **(a, b, e, f)**, is shown as black contours ($\pm 5, 10\,\mathrm{m\,s^{-1}}$). **(g, h)** The anomalous 100 hPa meridional eddy heat flux is shaded, and positive (negative) contours of $\pm 50\,\mathrm{K\,m\,s^{-1}}$ from Fig. 3 are highlighted as solid purple (dashed green) lines. Here, the prime symbol denotes the deviation from the zonal mean (or eddy component), while the sub-indexes c and a denote the climatological mean and anomalies.

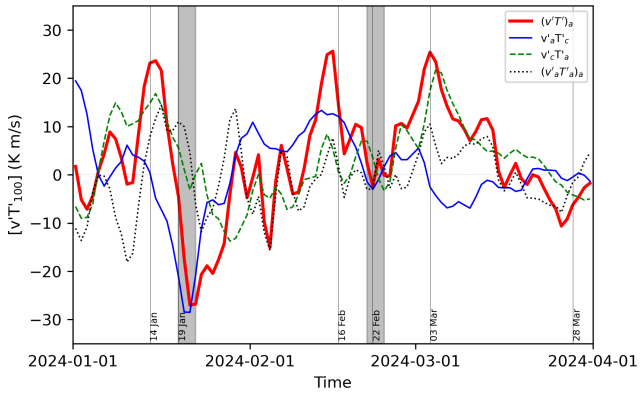

Figure 5. Time series of the anomalous 100 hPa meridional eddy heat flux (Eq. 3), area averaged poleward of 45° N (thick red), and its components, $v'_aT'_c$ (solid blue), $v'_cT'_a$ (dashed green), and $(v'_aT'_a)_a$ (dotted black). The sub-indexes c and a denote the climatological mean and anomalies. The vertical gray stripes indicate the window of 5–8 d after the onset, as in Fig. 4.

ever, Rao et al. (2019) showed that SSWs take place more frequently in moderate El Niño winters. The interconnections between the QBO and ENSO phases can modulate the overall probability of SSW events. The 11-year solar cycle also affects the occurrence of sudden stratospheric warmings (SSWs). During the solar maximum, SSWs tend to be more frequent due to the weaker and more disturbed polar vortex. The effect is the opposite during the solar minimum, where the polar vortex is generally stronger and more stable, reducing the chances of SSW events. Furthermore, the influence of the solar cycle can interact with other factors like the QBO and ENSO, further modulating the SSW likelihood. In addition, enhanced Eurasian snow cover has been reported as a factor influencing polar vortex variability (e.g., Cohen et al., 2007; Garfinkel et al., 2010; Henderson et al., 2018; Lü et al., 2020). Although the exact mechanism is not yet fully understood, the latest understanding of snow–stratosphere coupling is that snow anomalies, through their cooling effect, may contribute to regional modifications in near-surface temperature gradients and hence land–sea thermal contrasts that are conducive to the generation of PWs. For a summary of favorable conditions for five SSWs in the last decade (2014–2024), see Table 1 in Rao et al. (2025).

In the winter of 2023/24, the QBO was in its easterly phase, while ENSO was in the El Niño phase (see Qian et al., 2024, for details). At the same time, solar cycle 25 approached its maximum, predicted for July 2025 according to the NOAA Space Weather Prediction Center. In addition, Vorobeva and Orsolini (2024) showed that the Northern Hemisphere snow cover exceeded its climatological mean by approximately 1 standard deviation in the second half of January 2024. Each of these external factors has previously been shown to increase the likelihood of SSWs, collectively creating favorable conditions for their occurrence.

Complementing the recent studies of stratospheric dynamics in the winter of 2023/24 by Qian et al. (2024), Lee et al. (2025), and Rao et al. (2025), we conducted a detailed investigation into the mechanisms governing the duration and termination of SSWs, as it remains unclear why some SSWs develop into long-lived events while others terminate rapidly. Using the ERA5 reanalysis data and the SSW definition based on the polar-cap-averaged U, we identify three major SSW events in the winter of 2023/24. For all three SSWs, our analysis demonstrates that blocking highs that developed over the PW ridges played a crucial role in enhancing PW activity prior to onset. The first SSW occurred in January 2024, lasting from the 14th to the 19th. Its rapid termination and the subsequent recovery of the polar vortex are linked to a developing high-pressure system over the PW trough in the western North Pacific. The second SSW took place in February 2025, from the 16th to 22nd. We find that its abrupt termination was influenced (though not exclusively driven) by a westward-propagating BH that migrated over the PW trough into the Far East. The third SSW occurred in March 2024, lasting from the 3rd to the 28th, making it a long-duration canonical SSW event. Analysis of the tropospheric forcing conditions reveals that a persistent large-scale high-pressure system over the PW ridge in northern Europe sustained enhanced upward PW activity, favoring the development of an extended SSW. This study highlights that subtle synoptic developments in distant oceanic basins condition the specific evolution of SSWs. In particular, synoptic developments over the Far East and the North Pacific play an important role in the termination of short events.

Data availability. Hourly ERA5 data on pressure levels from 1940 to the present are available from the Climate Data Store website via https://doi.org/10.24381/cds.bd0915c6 (Hersbach et al., 2023).

Author contributions. EV and YO contributed equally to the conception of this study. EV analyzed the data and made all figures.

Competing interests. The contact author has declared that neither of the authors has any competing interests.

Disclaimer. Publisher's note: Copernicus Publications remains neutral with regard to jurisdictional claims made in the text, published maps, institutional affiliations, or any other geographical representation in this paper. While Copernicus Publications makes every effort to include appropriate place names, the final responsibility lies with the authors.

Acknowledgements. The authors thank the ECMWF for providing open-access data for this study.

Review statement. This paper was edited by Amy Butler and reviewed by two anonymous referees.

References

Andrews, D. G., Holton, J. R., and Leovy, C. B.: Middle Atmosphere Dynamics, 40, Academic Press, ISBN 978-0-12-058575-5, 1987.

Ayarzagüena, B., Orsolini, Y. J., Langematz, U., Abalichin, J., and Kubin, A.: The relevance of the location of blocking highs for stratospheric variability in a changing climate, J. Climate, 28, 531–549, https://doi.org/10.1175/JCLI-D-14-00210.1, 2015.

Baldwin, M. P., Ayarzagüena, B., Birner, T., Butchart, N., Butler, A. H., Charlton-Perez, A. J., Domeisen, D. I. V., Garfinkel, C. I., Garny, H., Gerber, E. P., Hegglin, M. I., Langematz, U., and Pedatella, N. M.: Sudden stratospheric warmings, Rev. Geophys., 59, e2020RG000708, https://doi.org/10.1029/2020RG000708, 2021.

Bancalá, S., Krüger, K., and Giorgetta, M.: The preconditioning of major sudden stratospheric warmings, J. Geophys. Res.-Atmos., 117, D04101, https://doi.org/10.1029/2011JD016769, 2012.

Bell, B., Hersbach, H., Simmons, A., Berrisford, P., Dahlgren, P., Horányi, A., Muñoz-Sabater, J., Nicolas, J., Radu, R., Schepers, D., Soci, C., Villaume, S., Bidlot, J.-R., Haimberger, L., Woollen, J., Buontempo, C., and Thépaut, J.-N.: The ERA5 global reanalysis: preliminary extension to 1950, Q. J. Roy. Meteor. Soc., 147, 4186–4227, https://doi.org/10.1002/qj.4174, 2021.

Butler, A. H. and Gerber, E. P.: Optimizing the definition of a sudden stratospheric warming, J. Climate, 31, 2337–2344, https://doi.org/10.1175/JCLI-D-17-0648.1, 2018.

Butler, A. H., Seidel, D. J., Hardiman, S. C., Butchart, N., Birner, T., and Match, A.: Defining sudden stratospheric warmings, B. Am. Meteorol. Soc., 96, 1913–1928, https://doi.org/10.1175/BAMS-D-13-00173.1, 2015.

Butler, A. H., Sjoberg, J. P., Seidel, D. J., and Rosenlof, K. H.: A sudden stratospheric warming compendium, Earth Syst. Sci. Data, 9, 63–76, https://doi.org/10.5194/essd-9-63-2017, 2017.

Charlton, A. J. and Polvani, L. M.: A new look at stratospheric sudden warmings. Part I: Climatology and modeling benchmarks, J. Climate, 20, 449–469, https://doi.org/10.1175/JCLI3996.1, 2007.

Cohen, J., Barlow, M., Kushner, P. J., and Saito, K.: Stratosphere–troposphere coupling and links with Eurasian land surface variability, J. Climate, 20, 5335–5343, https://doi.org/10.1175/2007JCLI1725.1, 2007.

Coy, L., Nash, E. R., and Newman, P. A.: Meteorology of the polar vortex: Spring 1997, Geophys. Res. Lett., 24, 2693–2696, https://doi.org/10.1029/97GL52832, 1997.

Domeisen, D. I.: Estimating the frequency of sudden stratospheric warming events from surface observations of the North Atlantic Oscillation, J. Geophys. Res.-Atmos., 124, 3180–3194, https://doi.org/10.1029/2018JD030077, 2019.

Garfinkel, C. I., Hartmann, D. L., and Sassi, F.: Tropospheric precursors of anomalous Northern Hemisphere stratospheric polar vortices, J. Climate, 23, 3282–3299, https://doi.org/10.1175/2010JCLI3010.1, 2010.

Henderson, G. R., Peings, Y., Furtado, J. C., and Kushner, P. J.: Snow–atmosphere coupling in the Northern Hemisphere, Nat. Clim. Change, 8, 954–963, https://doi.org/10.1038/s41558-018-0295-6, 2018.

Hersbach, H., Bell, B., Berrisford, P., Hirahara, S., Horányi, A., Muñoz-Sabater, J., Nicolas, J., Peubey, C., Radu, R., Schepers, D., Simmons, A., Soci, C., Abdalla, S., Abellan, X., Balsamo, G., Bechtold, P., Biavati, G., Bidlot, J., Bonavita, M., De Chiara, G., Dahlgren, P., Dee, D., Diamantakis, M., Dragani, R., Flemming, J., Forbes, R., Fuentes, M., Geer, A., Haimberger, L., Healy, S., Hogan, R. J., Hólm, E., Janisková, M., Keeley, S., Laloyaux, P., Lopez, P., Lupu, C., Radnoti, G., de Rosnay, P., Rozum, I., Vamborg, F., Villaume, S., and Thépaut, J.-N.: The ERA5 global reanalysis, Q. J. Roy. Meteor. Soc., 146, 1999–2049, https://doi.org/10.1002/qj.3803, 2020.

Hersbach, H., Bell, B., Berrisford, P., Biavati, G., Horányi, A., Muñoz Sabater, J., Nicolas, J., Peubey, C., Radu, R., Rozum, I., Schepers, D., Simmons, A., Soci, C., Dee, D., and Thépaut, J.-N.: ERA5 hourly data on pressure levels from 1940 to present, Copernicus Climate Change Service (C3S) Climate Data Store (CDS) [data set], https://doi.org/10.24381/cds.bd0915c6, 2023.

Hinssen, Y. B. L. and Ambaum, M. H. P.: Relation between the 100-hPa heat flux and stratospheric potential vorticity, J. Atmos. Sci., 67, 4017–4027, https://doi.org/10.1175/2010JAS3569.1, 2010.

Ineson, S., Dunstone, N. J., Scaife, A. A., Andrews, M. B., Lockwood, J. F., and Pang, B.: Statistics of sudden stratospheric warmings using a large model ensemble, Atmos. Sci. Lett., 25, e1202, https://doi.org/10.1002/asl.1202, 2024.

Karpechko, A. Y., Hitchcock, P., Peters, D. H., and Schneidereit, A.: Predictability of downward propagation of major sudden stratospheric warmings, Q. J. Roy. Meteor. Soc., 143, 1459–1470, https://doi.org/10.1002/qj.3017, 2017.

Kolstad, E. W., Breiteig, T., and Scaife, A. A.: The association between stratospheric weak polar vortex events and cold air outbreaks in the Northern Hemisphere, Q. J. Roy. Meteor. Soc., 136, 886–893, https://doi.org/10.1002/qj.620, 2010.

Lee, S. H., Butler, A. H., and Manney, G. L.: Two major sudden stratospheric warmings during winter 2023/2024, Weather, 80, 45–53, https://doi.org/10.1002/wea.7656, 2025.

Liang, Z., Rao, J., Guo, D., and Lu, Q.: Simulation and projection of the sudden stratospheric warming events in different scenarios by CESM2-WACCM, Clim. Dynam., 59, 3741–3761, https://doi.org/10.1007/s00382-022-06293-2, 2022.

Limpasuvan, V., Thompson, D. W. J., and Hartmann, D. L.: The life cycle of the Northern Hemisphere sudden stratospheric warmings, J. Climate, 17, 2584–2596, https://doi.org/10.1175/1520-0442(2004)017<2584:TLCOTN>2.0.CO;2, 2004.

Limpasuvan, V., Orsolini, Y. J., Chandran, A., Garcia, R. R., and Smith, A. K.: On the composite response of the MLT to major sudden stratospheric warming events with elevated stratopause, J. Geophys. Res.-Atmos., 121, 4518–4537, https://doi.org/10.1002/2015JD024401, 2016.

Lü, Z., Li, F., Orsolini, Y. J., Gao, Y., and He, S.: Understanding of european cold extremes, sudden stratospheric warming, and siberian snow accumulation in the winter of 2017/18, J. Climate, 33, 527–545, https://doi.org/10.1175/JCLI-D-18-0861.1, 2020.

Martius, O., Polvani, L. M., and Davies, H. C.: Blocking precursors to stratospheric sudden warming events, Geophys. Res. Lett., 36, L14806, https://doi.org/10.1029/2009GL038776, 2009.

Matsuno, T.: Vertical propagation of stationary planetary waves in the winter Northern Hemisphere, J. Atmos. Sci., 27, 871–883, https://doi.org/10.1175/1520-0469(1970)027<0871:VPOSPW>2.0.CO;2, 1970.

Matthias, V., Dörnbrack, A., and Stober, G.: The extraordinarily strong and cold polar vortex in the early northern winter 2015/2016, Geophys. Res. Lett., 43, 12287–12294, https://doi.org/10.1002/2016GL071676, 2016.

Newman, P. A. and Nash, E. R.: Quantifying the wave driving of the stratosphere, J. Geophys. Res.-Atmos., 105, 12485–12497, https://doi.org/10.1029/1999JD901191, 2000.

Newman, P. A., Nash, E. R., and Rosenfield, J. E.: What controls the temperature of the Arctic stratosphere during the spring?, J. Geophys. Res.-Atmos., 106, 19999–20010, https://doi.org/10.1029/2000JD000061, 2001.

Nishii, K., Nakamura, H., and Miyasaka, T.: Modulations in the planetary wave field induced by upward-propagating Rossby wave packets prior to stratospheric sudden warming events: a case-study, Q. J. Roy. Meteor. Soc., 135, 39–52, https://doi.org/10.1002/qj.359, 2009.

Nishii, K., Nakamura, H., and Orsolini, Y. J.: Cooling of the wintertime Arctic stratosphere induced by the western Pacific teleconnection pattern, Geophys. Res. Lett., 37, L13805, https://doi.org/10.1029/2010GL043551, 2010.

Nishii, K., Nakamura, H., and Orsolini, Y. J.: Geographical dependence observed in blocking high influence on the stratospheric variability through enhancement and suppression of upward planetary-wave propagation, J. Climate, 24, 6408–6423, https://doi.org/10.1175/JCLI-D-10-05021.1, 2011.

Orsolini, Y. J., Nishii, K., and Nakamura, H.: Duration and decay of Arctic stratospheric vortex events in the ECMWF seasonal forecast model, Q. J. Roy. Meteor. Soc., 144, 2876–2888, https://doi.org/10.1002/qj.3417, 2018.

Pedatella, N. M.: Influence of stratosphere polar vortex variability on the mesosphere, thermosphere, and ionosphere, J. Geophys. Res.-Space, 128, e2023JA031495, https://doi.org/10.1029/2023JA031495, 2023.

Polvani, L. M. and Waugh, D. W.: Upward wave activity flux as a precursor to extreme stratospheric events and subsequent anomalous surface weather regimes, J. Climate, 17, 3548–3554, https://doi.org/10.1175/1520-0442(2004)017%3C3548:UWAFAA%3E2.0.CO;2, 2004.

Qian, L., Rao, J., Ren, R., Shi, C., and Liu, S.: Enhanced stratosphere-troposphere and tropics-Arctic couplings in the 2023/24 winter, Communications Earth and Environment, 5, 631, https://doi.org/10.1038/s43247-024-01812-x, 2024.

Qin, Y., Gu, S.-Y., Dou, X., Wei, Y., Liu, Y., and Chen, H.: First observation of dominant quasi-two-day wave with westward zonal wavenumber 3 at the December solstice during austral summer: links to persistent winter stratopause warming, Geophys. Res. Lett., 52, e2024GL113698, https://doi.org/10.1029/2024GL113698, 2025.

Rao, J. and Garfinkel, C. I.: CMIP5/6 models project little change in the statistical characteristics of sudden stratospheric warmings in the 21st century, Environ. Res. Lett., 16, 034024, https://doi.org/10.1088/1748-9326/abd4fe, 2021.

Rao, J., Garfinkel, C. I., Chen, H., and White, I. P.: The 2019 New Year stratospheric sudden warming and its real-time predictions in multiple S2S models, J. Geophys. Res.-Atmos., 124, 11155–11174, https://doi.org/10.1029/2019JD030826, 2019.

Rao, J., Zhang, X., Lu, Q., and Liu, S.: Prediction of near-surface conditions following the 2023/24 sudden stratospheric warming by the S2S project models, Atmos. Res., 315, 107882, https://doi.org/10.1016/j.atmosres.2024.107882, 2025.

Shepherd, M. G., Beagley, S. R., and Fomichev, V. I.: Stratospheric warming influence on the mesosphere/lower thermosphere as seen by the extended CMAM, Ann. Geophys., 32, 589–608, https://doi.org/10.5194/angeo-32-589-2014, 2014.

Sjoberg, J. P. and Birner, T.: Transient tropospheric forcing of sudden stratospheric warmings, J. Atmos. Sci., 69, 3420–3432, https://doi.org/10.1175/JAS-D-11-0195.1, 2012.

Vorobeva, E. and Orsolini, Y.: A series of major sudden stratospheric warming events in winter 2023/2024, EMS Annual Meeting 2024, Barcelona, Spain, 1–6 Sep 2024, EMS2024-163, https://doi.org/10.5194/ems2024-163, 2024.

Waugh, D. W. and Polvani, L. M.: Stratospheric Polar Vortices, Chap. 3, American Geophysical Union (AGU), https://doi.org/10.1002/9781118666630.ch3, ISBN 9781118666630 (Online), 43–57, 2010.

Woollings, T., Charlton-Perez, A., Ineson, S., Marshall, A. G., and Masato, G.: Associations between stratospheric variability and tropospheric blocking, J. Geophys. Res.-Atmos., 115, D06108, https://doi.org/10.1029/2009JD012742, 2010.